FULL PAPER

Dalton
www.rsc.org/dalton

Synthesis, crystal structure and mass transport properties of novel thallium ion precursors for MOCVD applications

Graziella Malandrino,[a] Anna M. Borzì,[a] Francesco Castelli,[a] Ignazio L. Fragalà,*[a] Walter Dastrù,[b] Roberto Gobetto,[b] Patrizia Rossi[c] and Paolo Dapporto[c]

[a] *Dipartimento di Scienze Chimiche, Universita' di Catania, I.N.S.T.M. UdR di Catania, Viale Andrea Doria 6, I-95125 Catania, Italy*

[b] *Dipartimento di Chimica Inorganica, Chimica Fisica e Chimica dei Materiali, Università di Torino, Via Pietro Giuria 7, I-10125 Torino, Italy*

[c] *Dipartimento Energetica, Via Santa Marta 3, I-50139 Firenze, Italy*

Received 30th July 2002, Accepted 25th November 2002
First published as an Advance Article on the web 2nd January 2003

The reaction of Tl_2CO_3 with 1,1,1,5,5,5-hexafluoro-2,4-pentanedione (Hhfa) and diglyme $\{CH_3O(CH_2CH_2O)_2CH_3\}$ or tetraglyme $\{CH_3O(CH_2CH_2O)_4CH_3\}$ in dichloromethane yields the anhydrous, thermally and air stable, volatile Tl(hfa)·diglyme and Tl(hfa)·tetraglyme adducts. They have been characterized by single crystal X-ray diffraction, elemental analysis, ^{1}H and ^{13}C NMR, IR and mass spectroscopy. Thermal and mass-transport properties have been investigated using thermogravimetric and differential scanning calorimetric measurements. There is evidence that both precursors are very low melting and volatile, and can be used as liquid Tl sources. Both adducts have been successfully applied to metal–organic chemical vapor deposition of thallium containing films.

Introduction

The growing demand for novel precursors for metal–organic chemical vapor deposition (MOCVD)[1] of thallium based high critical temperature (H-*T*c) superconducting films (TlBaCaCuO)[2] has recently stimulated the design of novel co-ordination architectures and the search for new synthetic strategies.

High thermal stability upon evaporation, high vapor pressure and constant mass transport properties are prerequisite characteristics for MOCVD applications[3] and in this perspective several studies have been carried out on alkaline-earth metal sources.[4–9] So far, however, few studies have been reported on thallium precursors.[10]

The required properties for MOCVD applications have been found in several alkaline-earth β-diketonate complexes whose ligation environments are saturated with ancillary glyme ligands.[4–9] In particular, the successful combination of both ligands has resulted in highly volatile and thermally stable complexes where the glyme ligand precludes either water coordination or oligomerization, which often occurs with simple β-diketonates. Similarly, the glyme co-ordination to lanthanide β-diketonate complexes yielded thermally stable and volatile lanthanide precursors.[11–14]

In this perspective, there was enough motivation to attempt the same strategy for the Tl^+ ion and, in this paper, we report on the synthesis of two novel adducts, Tl(hfa)·diglyme (**1**) and Tl(hfa)·tetraglyme (**2**) (Hhfa = 1,1,1,5,5,5-hexafluoro-2,4-pentanedione, diglyme = bis(2-methoxyethyl)ether, tetraglyme = 2,5,8,11,14-pentaoxatetradecane) by a one-pot[15] reaction. The crystal structure of the diglyme adduct, physico-chemical and mass transport properties, and applications to the MOCVD of thallium-containing films are also reported.

Experimental

Materials

Commercial Tl_2CO_3, Hhfa, diglyme and tetraglyme were purchased from Aldrich and used without any further purification.

Physical measurements and instrumentation

Note that, particular attention has to be used in manipulating the thallium compounds. All the syntheses were carried out in a fume cupboard with adequate ventilation. The MOCVD reactor was allocated inside a totally filtered hood and liquid nitrogen traps were used to collect the unreacted precursor vapors. The pump exhausts were bubbled through three traps containing NaI solution to convert any Tl exhaust to insoluble yellow TlI.

Elemental microanalyses were performed at the Analytical Laboratories of the University of Catania. ^{1}H NMR spectra were recorded on a Varian Unity Inova 500 MHz spectrometer. The ^{13}C spectra were recorded on a JEOL EX 400 NMR spectrometer operating at 100.25 MHz. Infrared data were collected on a 684 Perkin-Elmer spectrometer from Nujol mulls between NaCl plates. Thermal measurements were made using a Mettler 3000 system equipped with a TG 50 thermobalance, a TC 10 processor and DSC 30 calorimeter. Masses of the samples were between 15 and 20 mg (TG) and 4 and 10 mg (DSC). Analyses were carried out under prepurified nitrogen using 10 °C min^{-1} (TG) and 5 °C min^{-1} (DSC) heating rates. FAB mass spectra were obtained using a Kratos MS 50 spectrometer.

Synthesis

Tl(hfa)·diglyme (1). Tl_2CO_3 (5.21 g, 11.11 mmol) was first suspended in dichloromethane (150 ml). Diglyme (2.84 g, 21.16 mmol) was added to the suspension. Upon addition of Hhfa (4.41 g, 21.19 mmol) the Tl_2CO_3 slightly dissolved. The excess of thallium carbonate was removed by filtration. After evaporation of the solvent, pale yellow crystals separated. They were recovered with hexane, collected by filtration and dried under vacuum. Yield 75%. Melting point of the crude product 39–42 °C. ^{1}H NMR (500 MHz, CD_2Cl_2): δ 3.36 (s, 6H, OCH_3), 3.54–3.66 (m, 8H, OCH_2), 5.68 (s, 1H, CH). ^{13}C NMR (100.25 MHz, CD_2Cl_2): δ 58.68 (s, OCH_3), 70.05 (s, OCH_2), 71.18 (s, OCH_2), 88.34 (s, CH), 118.42 (q, $^1J_{^{19}F-^{13}C}$ = 287.4 Hz, CF_3), 174.94 (q, $^2J_{^{19}F-^{13}C}$ = 30.7 Hz, CO). Anal. Calcd. for $TlC_{11}H_{15}O_5F_6$: C 24.21, H 2.77%. Found: C 24.24, H 2.53%.

Tl(hfa)·tetraglyme (2). Prepared as described for the diglyme adduct from 3.62 g (7.72 mmol) of Tl_2CO_3, 2.94 g, (14.13 mmol) of Hhfa and 3.14 g (14.13 mmol) of tetraglyme. Yield 88%. Melting point of the crude product 25–27 °C. ^{1}H NMR (500 MHz, CD_2Cl_2): δ 3.33 (s, 6H, OCH_3), 3.53 (m, 4H, OCH_2), 3.62 (m, 4H, OCH_2), 3.64 (s, 8H, OCH_2), 5.66 (s, 1H, CH). ^{13}C NMR (100.25 MHz, CD_2Cl_2): δ 58.27 (s, OCH_3), 70.06 (s, OCH_2), 70.12 (s, OCH_2), 70.15 (s, OCH_2), 71.63 (s, OCH_2), 86.03 (s, CH), 117.68 (q, $^1J_{^{19}F-^{13}C}$ = 287.5 Hz, CF_3), 172.99 (q,

DOI: 10.1039/b207470b

Table 1 Crystal data and structure refinement for Tl(hfa)·diglyme

Empirical formula	$C_{11}H_{15}F_6O_5Tl$
M	545.60
T/K	200
Crystal system	Orthorhombic
Space group	*Pnam*
a/Å	8.389(2)
b/Å	10.537(2)
c/Å	18.202(4)
V/Å^3	1609.0(6)
Z, d_{calc}/g cm^{-3}	4, 2.252
μ/mm^{-1}	20.114
F(000)	1024
Crystal size/mm	0.6 × 0.7 × 0.75
Reflections collected/unique	4640/1077 [R(int) = 0.0899]
Final R indices [$I>2\sigma(I)$]	$R1 = 0.0757$, $wR2 = 0.1771$
R indices (all data)	$R1 = 0.0786$, $wR2 = 0.1807$

${}^2J_{^{19}F-^{13}C}$ = 30.8 Hz, *C*O). Anal. Calcd. for $TlC_{15}H_{23}O_7F_6$: C 28.48, H 3.65%. Found: C 28.51, H 3.88%.

X-Ray structural determination of Tl(hfa)·diglyme. Data were collected, at 200 K, on a Siemens SMART CCD diffractometer equipped with rotating anode and controlled by SMART software.[16] The radiation used was Cu-K$_\alpha$ (λ = 1.5418 Å). Five settings of ω, narrow data 'frames', were collected for 0.3° increments in ω. A total of 2500 frames of data were collected affording a sphere of data. Data reduction was made with the SAINT 4.0 program.[17] The SADABS program[18] was used for the absorption correction. The crystal structure of **1** was solved by direct methods, using the SIR-97[19] program and subsequently refined by the full-matrix least-squares SHELX-97 program.[20] All the non-hydrogen atoms were refined anisotropically. The hydrogen atoms were introduced in calculated positions and refined accordingly to the linked atoms, the overall temperature factor converged to 0.06(1) Å^2. Crystal and structure refinement data are collected in Table 1. Geometrical calculations were performed by PARST97.[21] Molecular plots were produced by the ORTEP-3 program.[22]

CCDC reference number 190969.

See http://www.rsc.org/suppdata/dt/b2/b207470b/ for crystallographic data in CIF or other electronic format.

MOCVD experiments and film characterization

Tl_2O_3 films were prepared in a reduced pressure, horizontal hot-wall MOCVD reactor from the Tl(hfa)·tetraglyme precursor. Random YSZ (yttria stabilized zirconia) and glass substrates of about 10 × 10 mm^2 were used for the depositions. In this study, the precursor evaporation temperature was controlled in the 125–130 °C range and the substrate temperature was kept at 430 °C. Ar (150 sccm) and O_2 (900 sccm) flows were used as carrier and reaction gases, respectively. The mass flows were controlled with 1160 MKS flowmeters using an MKS 147 electronic control unit. Depositions were carried out for 60 minutes. The total pressure in the reactor was 14 Torr. The growth rate was about 1 µm h^{-1}.

θ–2θ X-ray diffraction (XRD) patterns were recorded on a Bruker-AXS D5005 θ–θ X-ray diffractometer, using Cu-K$_\alpha$ radiation operating at 40 kV and 30 mA. The atomic composition of the films was analyzed by energy dispersive X-ray analysis (EDX) using an IXRF windowless detector. The surface morphology was examined using a LEO Iridium 1450 scanning electron microscope (SEM).

Results and discussion

Synthesis and characterization

Tl(hfa)·diglyme and Tl(hfa)·tetraglyme were synthesized adopting a simple one-pot reaction involving Tl_2CO_3, hexafluoroacetylacetone and glyme in dichloromethane. The procedure can be used with common undried solvents and glassware and almost quantitatively yields the two water-free, air-stable, and volatile complexes. Adducts **1** and **2** have very low melting points (41 °C and 27 °C) and quantitatively evaporate from the melt at 120 and 125 °C (2 Torr), respectively. Unfortunately, the ultimate determination of the molecular structure by single crystal X-ray diffraction of the tetraglyme adduct is difficult due to the low melting point of the complex. Nevertheless, other physico-chemical studies, compared with data of closely related molecules, can be used to assess its structure.

X-Ray single crystal structures of Tl(hfa)·diglyme

The crystal structure of Tl(hfa)·diglyme consists of a polymeric array (Fig. 1) in which the oxygen atoms of two hfa and one diglyme link together two thallium ions. The ORTEP drawing of a Tl(hfa)·diglyme unit is reported in Fig. 2. The cation Tl$^+$ is coordinated by eight oxygen atoms: O1 and O1^a from the hfa molecule, O2, O3, O3^a [a: x, y, $-z + 3/2$] from the diglyme molecule, the symmetry related atoms O1^b, O2^b [b: $x + 1/2$, $-y + 1/2$, z], and finally by the symmetry related atom O1^c [c: $x + 1/2$, $-y + 1/2$, $-z + 3/2$]. Positional parameters and selected bond distances and angles are compiled in Table 2. The

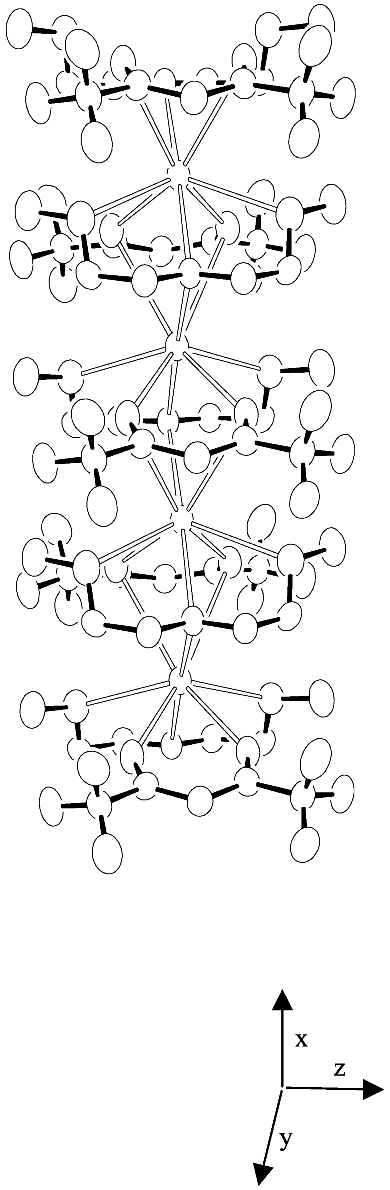

Fig. 1 ORTEP view of the polymeric structure of the Tl(hfa)·diglyme complex.

Table 2 Selected bond lengths (Å) and angles (°) for Tl(hfa)·diglyme

Tl1–O1	2.725(9)	Tl1–O1^{b}	3.304(9)
Tl1–O2	2.86(1)	Tl1–O2^{b}	3.25(1)
Tl1–O3	2.945(9)		
O1–Tl1–O2	92.0(2)	O2–Tl1–O3	59.3(2)
O1–Tl1–O3	125.3(3)	O2–Tl1–O1^{c}	112.7(2)
O1–Tl1–O1^{a}	63.8(3)	O2–Tl1–O2^{b}	170.6(3)
O1–Tl1–O3^{a}	71.3(3)	O2^{c}–Tl1–O1^{c}	75.6(2)
O1–Tl1–O1^{c}	155.0(3)	O3–Tl1–O1^{b}	117.5(2)
O1–Tl1–O1^{b}	116.4(3)	O3–Tl1–O3^{a}	116.5(2)
O1–Tl1–O2^{b}	80.0(2)	O3–Tl1–O2^{b}	121.6(2)
O1^{b}–Tl1–O1^{c}	51.7(2)	O3–Tl1–O1^{c}	73.8(2)

Symmetry transformations used to generate equivalent atoms: a x, y, $-z + 3/2$; b $x + 1/2$, $-y + 1/2$, z; c $x + 1/2$, $-y + 1/2$, $-z + 3/2$.

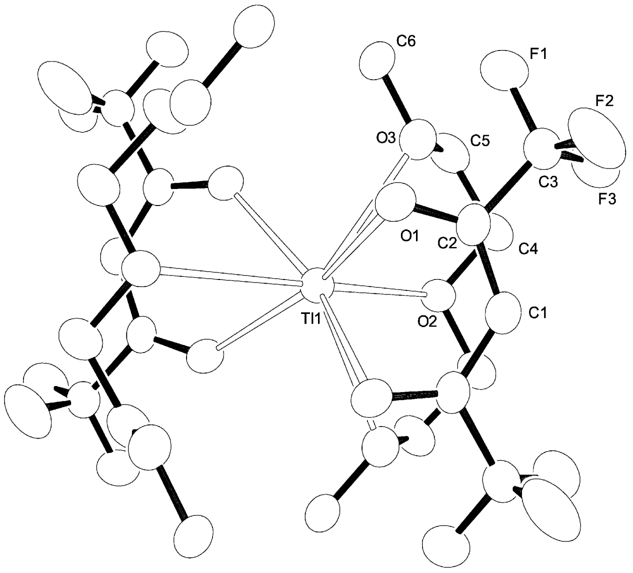

Fig. 2 ORTEP drawing of a Tl(hfa)·diglyme unit. CF_3 groups have been omitted for clarity.

coordination of thallium is irregular, with three Tl–O distances significantly longer than the other five (see Table 2). Present Tl–O bond distances can be grouped into primary (shorter than 3.1 Å) and secondary bonds (longer than 3.1 Å), and there is evidence that the former lies on the same side of the thallium ion. Therefore, the thallium lone pair is stereoactive, and the species represents a "5 + 3 coordination type" complex.[23,24]

The Tl ··· O and Tl ··· Tl distances in **1** have been compared with those found in structures of similar complexes (Cambridge Structural Database, CSD).[25] The Tl ··· O distances in **1** are significantly longer than those found in the CSD, in agreement with the trend observed in metal complexes involving acetylacetonate derivatives,[26] *i.e.* the distances are shorter when X = H than for X = F.

No coordination arrays involving the thallium cation and acyclic ethers have been found. Instead 23 thallium complexes with crown ethers have been retrieved.[27] The Tl ··· O (diglyme) distances currently found are in agreement with those reported for the crown ether adducts.

Finally, the Tl ··· Tl distances in oxygen-bridged thallium complexes fall in the 3.712–4.585 Å range, in agreement with that found in the present adduct (Tl1 ··· Tl1^{b} : 4.241(1) Å).

The polymeric, chain structure found in **1** has also been compared with similar coordination environments, in possibly related metal complexes. Four silver complexes[28] have been found in the CSD.[25] In one case,[28b] the same minimal formula [Ag(hfa)·diglyme] has been found, but the silver complex is a dimer instead of a polymer. The Tl complex consists of a one-dimensional chain (Fig. 1) along the x axis with an xy glide plane. The coordination around the Tl1 atom involves, besides the three diglyme oxygen atoms, three symmetry related oxygen atoms O1^{b} and O1^{c}, belonging to the same hfa anion and O2^{b} of another diglyme molecule. On the other hand, the atoms O1, O1^{a} and O2 do not complete the coordination environment of Tl1^{b}, but that of the symmetry related thallium cation Tl1^{d} [d: $x - 1/2$, $-y + 1/2$, z] (see Scheme 1).

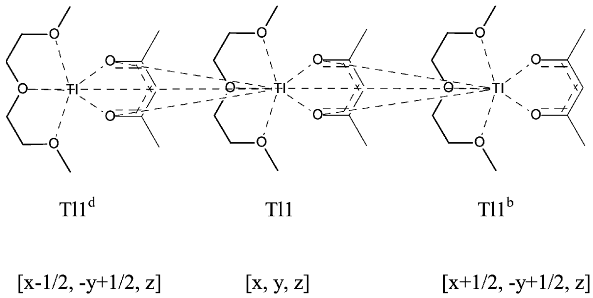

Scheme 1

Physico-chemical characterization

The IR spectra of the adducts **1** and **2** are reported in Fig. 3. The spectrum of adduct **1** (Nujol mull) does not show any bands around 3600 cm^{-1}, and therefore provides evidence of no H_2O molecules coordinated to the metal ion. The spectrum of adduct **2** has been recorded as a neat sample and shows a small feature around 3600 cm^{-1}, which can be attributed to O–H stretching, likely arising from contamination of the as-synthesized adduct with H_2O produced during the reaction. Note that, adduct **2** is a liquid at room temperature and has been obtained by evaporation of the solvent.

As found in analogous complexes,[11–14] C=O stretching is similarly observed at 1660 cm^{-1}, while C=C stretching is associated with the absorption at 1520 cm^{-1}. The broad band observed in the 1000–1300 cm^{-1} range may be associated with absorptions of the polyether C–O bending and/or stretching overlapped with the C–F stretching. It can be noted, in addition, that the spectrum of adduct **2** shows peaks at 1030 and 850 cm^{-1}, which may be considered fingerprints of the glyme coordination to metal ions, as already observed for homologous compounds.[14]

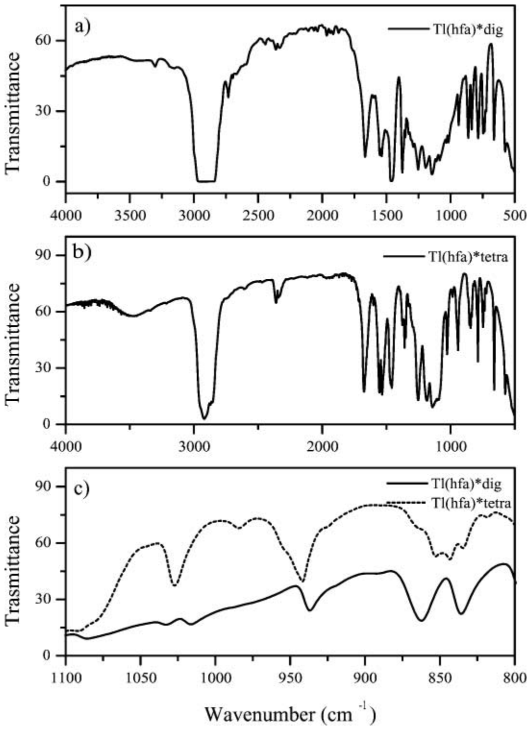

Fig. 3 IR-spectra of both Tl(hfa)·diglyme and Tl(hfa)·tetraglyme adducts as Nujol mulls.

Table 3 Major peaks in the mass spectra of adducts **1** and **2**[a]

Sample	Tl^+	$[M - hfa]^+$	$[Tl_2F]^+$	$[Tl_2{\cdot}L{\cdot}F]^+$	$[Tl_3F_2]^+$	$[Tl_4F_3]^+$	$[Tl_5F_4]^+$	$[Tl_6F_5]^+$
Tl(hfa)·diglyme	205	339	429		648	874	1098	1321
Tl(hfa)·tetraglyme		427		651				

[a] M = Molecular ion peak. L = tetraglyme. The given *m*/*z* ratios are related to the isotope ^{205}Tl.

Note that, the corresponding peaks in adduct **1** are both split into double peaks. This may be likely associated with the two different C–O stretchings for the diglyme oxygen atoms: O3 and O3^a (see Scheme 1), which coordinate only one thallium ion and O2, which coordinates two thallium ions.

The FAB spectra of the adducts do not show the molecular ion peaks. The spectrum of adduct **1** shows a considerable number of peaks which can be associated with the formation of Tl–F clusters of various stoichiometries as well as with the ion $[M - hfa]^+$. A complete assignment is reported in Table 3. It is worth noting that the observed isotopic pattern matches well with the number of thallium ions present in the clusters. In the spectrum of **2** (Table 3) the observed Tl isotopic pattern and the ^{13}C isotopic peak in the envelopes at 427 and 648 *m*/*z* can be accounted for by the overlapping of the fragment peaks $[M - hfa]^+$ and $[Tl_2{\cdot}L{\cdot}F]^+$ with those of $[Tl_2F]^+$ and $[Tl_3F_2]^+$, respectively. In the lower mass region, the most abundant peaks correspond, in both cases, to the $[Tl]^+$ ion.

The NMR data can give, additionally, useful insights on the coordination of glyme ancillary ligands in terms of the number of oxygen atoms coordinated to the metal ion, and in some cases, it can give interesting information on the fluxional processes in the solid state.[13,29] The ^{1}H NMR spectrum (CD_2Cl_2) of adduct **1** shows a singlet (5.68 ppm) associated with the ring proton of the hfa ligand. The methyl groups (**a**[30] protons) of the diglyme are observed as a singlet at 3.36 ppm. The **b** and **c** protons are responsible for the multiplet structure centered around 3.66 ppm. The ^{13}C NMR (CD_2Cl_2) spectrum shows resonances associated with the coordinated hfa ligands at 88.34 (s, *C*H), 118.42 ($J_{^{13}C-^{19}F}$ = 287.4 Hz, quartet, *C*F_3) and 174.94 ppm ($J_{^{13}C-^{19}F}$ = 30.7 Hz, quartet, *C*OCF_3), while resonances associated with the coordinated diglyme are detected at 58.68 (s, O*C*H_3, **a**), 70.05 (s, O*C*H_2, **b**), 71.18 ppm (s, O*C*H_2, **c**).

The ^{1}H NMR spectrum (CD_2Cl_2) of adduct **2** shows a singlet (5.66 ppm) associated with the ring proton of the hfa ligand. The resonances associated with the tetraglyme ligand consist of a broad peak at 3.64 ppm due to internal CH_2 groups, a unique resonance at 3.33 ppm due to the methoxy groups, and the typical AA′BB′ pattern centered at 3.62 and 3.53 ppm, that can be assigned to the external CH_2CH_2 units of the tetraglyme ligand. This pattern agrees well with a rigidity in the coordination of the five O-donor atoms of the tetraglyme. This general pattern, in addition, is almost identical to that observed in the spectrum of the La(hfa)$_3$·tetraglyme adduct, whose single crystal X-ray diffraction data provide an indication of partial metal coordination involving only four of the five oxygen atoms, even though, in the related ^{1}H NMR spectrum, the methyl groups of the tetraglyme ligand give rise to a single resonance at 3.34 ppm, thus implying a fast dynamic exchange of the methoxy groups in solution.[13]

In this context, the variable temperature ^{13}C NMR data can give useful insights into the glyme coordination in adduct **2**. The ^{13}C NMR spectrum (CD_2Cl_2) of **2** recorded at room temperature (RT) shows six resonances at 58.27 (s, O*C*H_3, **a**), 70.06 (s, O*C*H_2, **b**), 70.12 (s, O*C*H_2, **c**), 70.15 (s, O*C*H_2, **d**), 71.63 (s, O*C*H_2, **e**) and 86.03 ppm (*C*H), and two quartets centered at 117.68 ppm ($J_{^{13}C-^{19}F}$ = 287.5 Hz, *C*F_3) and 172.99 ppm ($J_{^{13}C-^{19}F}$ = 30.8 Hz, *C*OCF_3), respectively. The resonances are similar to those previously reported for the lanthanum homologue.[13] In both cases, the reduced number of differing resonances for the tetraglyme and the hfa ligand is in agreement with the presence of symmetry within the coordination cage of either the thallium or the lanthanum atoms. It could, therefore, be suggested that a fast dynamic exchange process involving coordinated and uncoordinated methoxy groups of the tetraglyme moiety is occurring. The low temperature ^{13}C NMR spectra of the Tl and La tetraglyme adducts, recorded at −70 °C, do not show any significant change in the overall resonance pattern, except for some minor shifts due to the temperature variation. Upon lowering the temperature to −90 °C, the resonances of the lanthanum adduct at ≈58 and at ≈70 ppm are significantly broadened compared to those found in the thallium adduct (Fig. 4). This observation points to a reduced dynamic exchange in the case of the lanthanum adduct and suggests a partial coordination of tetraglyme in accordance with single crystal X-ray data.[13]

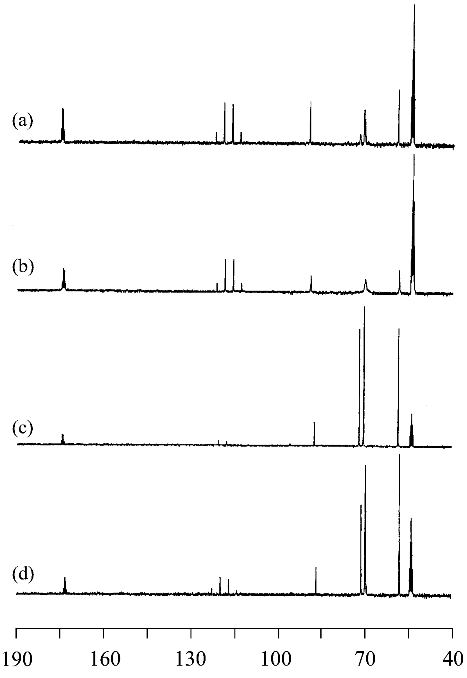

Fig. 4 ^{13}C spectra recorded at 100.25 MHz of: (a) La(hfa)$_3$·tetraglyme at RT; (b) La(hfa)$_3$·tetraglyme at −90 °C; (c) Tl(hfa)·tetraglyme at RT; (d) Tl(hfa)·tetraglyme at −90 °C.

For the tetraglyme Tl adduct the ^{13}C resonances also remain sharp at the lowest attainable temperature (−90 °C). These data, together with simple considerations on the value of the Tl^+ ionic radius (1.40 Å) and the coordination number found for the diglyme adduct by single crystal X-ray diffraction (*vide infra*), suggest a complete coordination of all the oxygen atoms of the polyether in agreement with the coordination environment around the Tl^+ ion as shown in Scheme 2.

Note that in the proposed structure, seven O-donor atoms are bonded to the metal ion and the hfa ligand occupies two equivalent equatorial sites of a pentagonal bipyramid or of a monocapped octahedron. Nevertheless, a lower activation energy for a dynamic motion involving coordinated and uncoordinated methoxy groups in the case of an octahedral Tl compound cannot be ruled out.

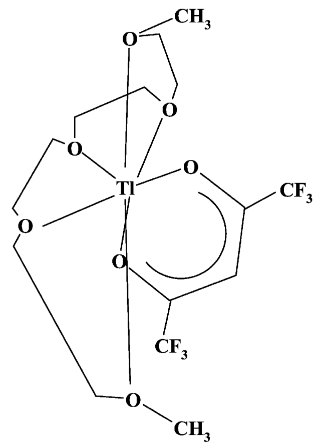

Scheme 2

Mass transport properties

Thermogravimetric (TG) analyses and atmospheric pressure TG vaporization rate data of adducts **1** and **2** are reported in Figs. 5 and 6, respectively. The TG curves show singular sublimation steps in the range 40–220 °C with an 8% residue left at 270 °C and 90–230 °C with a 3% residue left at 270 °C, respectively. 50% weight losses are observed (under the present operating conditions) at 152 °C and 161 °C for **1** and **2**, respectively. The linear behavior of the TG atmospheric pressure vaporization rates (Fig. 6) of adducts **1** and **2** indicate that both adducts are thermally stable and, therefore, represent potentially interesting precursors for MOCVD applications.

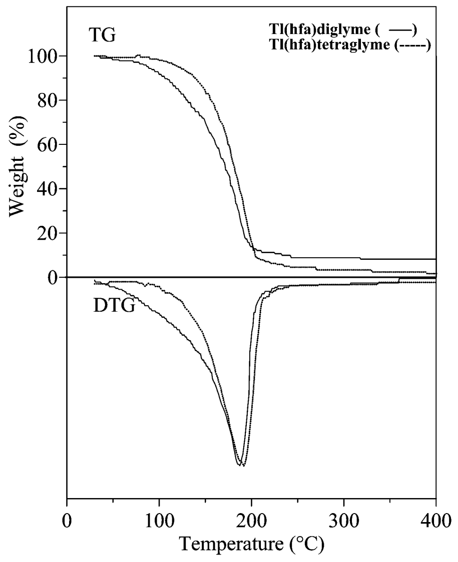

Fig. 5 Thermogravimetric curves of Tl(hfa)•diglyme and Tl(hfa)•tetraglyme adducts.

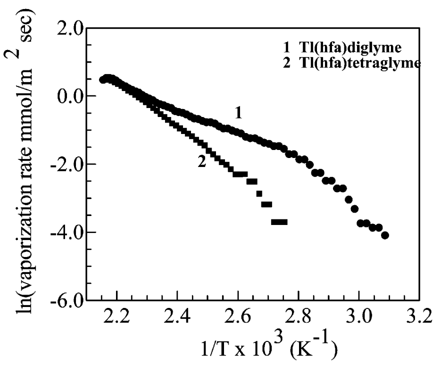

Fig. 6 Atmospheric pressure TG vaporization rate data of adducts **1** and **2** as a function of temperature.

The differential scanning calorimetric (DSC) data (Fig. 7) of the present adducts, carried out under atmospheric pressure, show two endothermic peaks at 43 °C and 27 °C for adducts **1** and **2**, respectively, and two exothermic peaks in the 160–190 °C (adduct **1**) and 190–210 °C (adduct **2**) temperature ranges. The endothermic peaks are associated with the melting of the adducts and match the melting points observed with the Koeffler microscope. The higher temperature peaks are possibly associated with exothermic processes overlapping the evaporation processes.

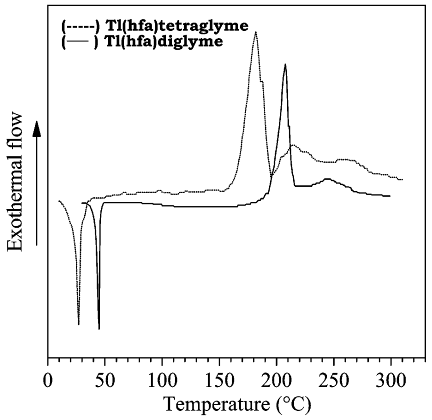

Fig. 7 DSC curves of the Tl(hfa)•diglyme and Tl(hfa)•tetraglyme adducts.

MOCVD depositions

Preliminary low-pressure MOCVD experiments, carried out on glass and random YSZ substrates 10 × 10 mm^2 with either the Tl(hfa)•diglyme or the Tl(hfa)•tetraglyme adducts, yielded thallium-containing films. Adduct **2** proved to be a "user-friendly" precursor for the deposition of thallium-containing films since its lower melting point (27 °C) allows manipulation (after mild heating).

The chemical nature of the deposited films has been investigated by X-ray diffraction (XRD) measurements and by energy dispersive X-ray analysis (EDX).

The XRD pattern of a film deposited at 430 °C and 14 Torr (Fig. 8a) shows reflections that can be indexed as Tl_2O_3.[31] The observed intensities are different from those reported for a polycrystalline powder, thus suggesting that some texturing occurs upon growth. The EDX spectrum, reported in Fig. 8b, shows the presence of the X-ray peaks Tl Mα and Tl Mβ at 2.265 and 2.360 keV, respectively, and of the O Kα peak at 0.570 keV. The peak observed at 2.040 keV is attributable to the substrate Zr Lα peak. Note that, the use of a windowless EDX detector allows the exclusion of any C and/or F contamination.

The SEM micrograph of the same sample shows a continuous film with a smooth and homogeneous surface with ≈5 μm grains.

Conclusions

Two novel adducts of the Tl^+ ion have been synthesized. They represent, to our knowledge, the first reported examples of stable β-diketonate adducts with glyme coordination to a group IIIA element. The TG and kinetic measurements indicate that both adducts possess mass transport properties suitable for MOCVD applications. In addition, preliminary MOCVD experiments, carried out with both adducts, clearly indicate that they represent promising MOCVD precursors for the deposition of Tl containing phases.

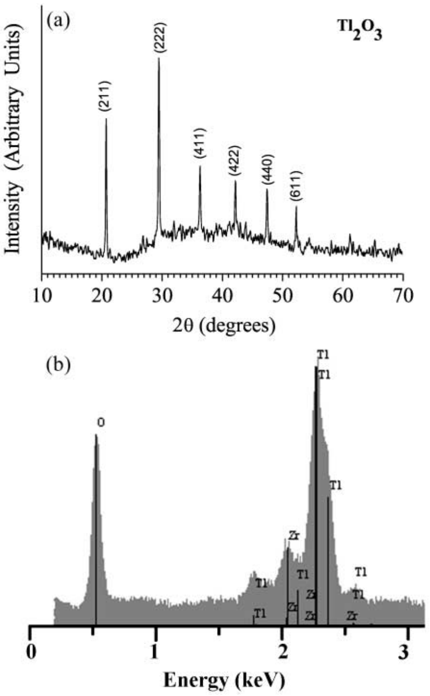

Fig. 8 X-Ray diffraction pattern (a) and energy dispersive X-ray analysis (b) of a Tl_2O_3 film deposited on random YSZ substrates (430 °C, 14 Torr) using the Tl(hfa)·tetraglyme adduct.

Acknowledgements

The authors thank the MIUR (Progetto Cluster 14 P.E. 2) for financial support.

References and notes

1 M. L. Hitchman and K. F. Jensen, *Chemical Vapor Deposition: Principles and Applications*, Academic Press, London, 1993.

2 (*a*) A. M. Hermann and J. V. Yakhmi, *Thallium Based High Temperature Superconductors*, Marcell Dekker Inc, New York, 1994; (*b*) B. J. Hinds, D. L. Schulz, D. A. Neumayer, B. Han, T. J. Marks, Y. Y. Wang, V. P. Dravid, J. L. Schindler, T. P. Hogan and C. R. Kannewurf, *Appl. Phys. Lett.*, 1994, **65**, 231.

3 J. T. Spencer, in *Progress in Inorganic Chemistry*, ed. K. D. Karlin, Wiley, New York, 1994, vol. 41, p. 145.

4 K. Timmer, K. I. M. A. Spee, A. Mackor, H. A. Meinema, A. L. Spek and P. Van der Sluis, *Inorg. Chim. Acta*, 1991, **190**, 109.

5 R. S. Drake, S. A. S. Miller and D. J. Williams, *Inorg. Chem.*, 1993, **32**, 3227.

6 G. Malandrino, I. L. Fragalà, D. A. Neumayer, C. L. Stern, B. J. Hinds and T. J. Marks, *J. Mater. Chem.*, 1994, **4**, 1061.

7 S. H. Shamlian, M. L. Hitchman, S. L. Cook and B. C. Richards, *J. Mater. Chem.*, 1994, **4**, 81.

8 G. Malandrino, F. Castelli and I. L. Fragalà, *Inorg. Chim. Acta*, 1994, **224**, 203.

9 D. A. Neumayer, D. B. Studebaker, B. J. Hinds, C. L. Stern and T. J. Marks, *Chem. Mater.*, 1994, **6**, 878.

10 (*a*) A. D. Berry, R. T. Holm, R. L. Mowery, N. H. Turner and M. Fatemi, *Chem. Mater.*, 1991, **3**, 72; (*b*) B. Krebs, A. Broemmelhaus, B. Kersting and M. Nienhaus, *Eur. J. Solid State Inorg. Chem.*, 1992, **29**, 167.

11 G. Malandrino, R. Licata, F. Castelli, I. L. Fragalà and C. Benelli, *Inorg. Chem.*, 1995, **34**, 6233.

12 (*a*) G. Malandrino, O. Incontro, F. Castelli, I. L. Fragalà and C. Benelli, *Chem. Mater.*, 1996, **8**, 1292; (*b*) G. Malandrino, R. Lo Nigro, F. Castelli, I. L. Fragalà and C. Benelli, *Adv. Mater. CVD*, 2000, **6**, 233.

13 G. Malandrino, I. L. Fragalà, S. Aime, W. Dastrù, R. Gobetto and C. Benelli, *J. Chem. Soc., Dalton Trans.*, 1998, 1509.

14 G. Malandrino, C. Benelli, F. Castelli and I. L. Fragalà, *Chem. Mater.*, 1998, **10**, 3434.

15 The term one-pot indicates an easy reaction carried out in a single step.

16 SMART, Area-Detector Integration Software, Siemens Industrial Automation, Inc., Madison, WI, 1995.

17 SAINT, Version 4.0, Siemens Industrial Automation, Inc., Madison, WI, 1995.

18 G. M. Sheldrick, SADABS, University of Göttingen, Germany, 1997.

19 A. Altomare, G. L. Cascarano, C. Giacovazzo, A. Guagliardi, M. C. Burla, G. Polidori and M. Cavalli, *J. Appl. Crystallogr.*, 1999, **32**, 115.

20 G. M. Sheldrick, SHELX 97, University of Göttingen, Germany, 1997.

21 M. Nardelli, *Comput. Chem.*, 1983, **7**, 95.

22 L. J. Farruggia, *J. Appl. Phys.*, 1997, **30**, 565.

23 I. D. Brown and R. Faggiani, *Acta Crystallogr., Sect. B*, 1980, **36**, 1802.

24 P. P. Toledano, M. Touboul and P. Herpin, *Acta Crystallogr., Sect. B*, 1976, **32**, 1859.

25 F. H. Allen and O. Kennard, Cambridge Structural Database, *J. Chem. Soc., Perkin Trans.*, 1989, **2**, 1131.

26 (*a*) R. P. Hughes, A. L. Rheingold and M. B. Allen, private communication, 1996; (*b*) E. J. Fernandez, P. G. Jones, A. Laguna and A. Mendia, *Inorg. Chim. Acta*, 1994, 229.

27 (*a*) V. A. Trush, K. V. Domasevitch, V. M. Amirkhanov and J. Sieler, *Z. Naturforsch., Teil B*, 1999, **54**, 451; (*b*) Yu. A. Manskaya, K. V. Domasevich, V. R. Polyakov, V. N. Kokozei and O. Yu. Vasil'eva, *Zh. Obshch. Khim.*, 1999, **69**, 101; (*c*) I. A. Kahwa, D. Miller, M. Mitchel, F. R. Fronczek, R. G. Goodrich, D. J. Williams, C. A. O'Mahoney, A. M. Z. Slawin, S. V. Ley and C. J. Groombridge, *Inorg. Chem.*, 1992, **31**, 3963; (*d*) H. von Arnim, K. Dehnicke, K. Maczek and D. Fenske, *Z. Naturforsch., Teil B*, 1993, **48**, 1331; (*e*) P. J. Dutton, T. M. Fyles, V. V. Suresh, F. R. Fronczek and R. D. Gandour, *Can. J. Chem.*, 1993, **71**, 239.

28 (*a*) A. Bailey, T. S. Corbitt, M. J. Hampden-Smith, E. N. Duesler and T. T. Kodas, *Polyhedron*, 1993, **12**, 1785; (*b*) J. A. Darr, M. Poliakoff, A. J. Blake and Li Wan-Sheung, *Inorg. Chem.*, 1998, **37**, 5491; (*c*) P. Doppelt, T. H. Baum and L. Ricard, *Inorg. Chem.*, 1996, **35**, 1286.

29 R. Kumar, F. R. Fronczek, A. W. Maverick, A. J. Kim and L. G. Butler, *Chem. Mater.*, 1994, **6**, 587.

30 The following notation has been used: diglyme (CH_3(**a**)–O–CH_2(**b**)–CH_2(**c**))$_2$–O, tetraglyme (CH_3(**a**)–O–CH_2(**b**)–CH_2(**c**)–O–CH_2(**d**)–CH_2(**e**))$_2$–O.

31 JCPDS No. 5-584.